

Supporting Information

TiH Hydride Formed on Amorphous Black Titania: Unprecedented Active Species for Photocatalytic Hydrogen Evolution

Sicong Ma¹, Si-Da Huang¹, Ya-Hui Fang² and Zhi-Pan Liu^{1*}

¹ Collaborative Innovation Center of Chemistry for Energy Material, Shanghai Key Laboratory of Molecular Catalysis and Innovative Materials, Key Laboratory of Computational Physical Science, Department of Chemistry, Fudan University, Shanghai 200433, China

² School of Chemical and Environmental Engineering, Shanghai Institute of Technology, Shanghai 201418, China

Corresponding author email: zpliu@fudan.edu.cn

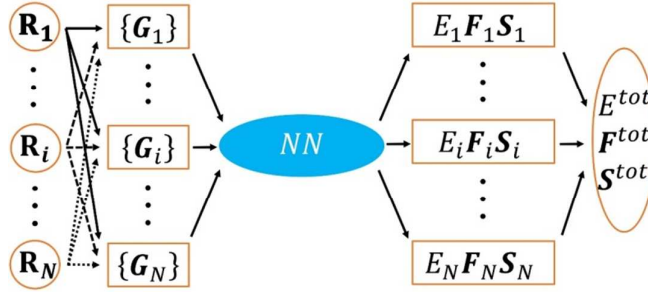
Table of Contents

1.1 Stochastic surface walking (SSW) global PES exploration using neural network (NN) potential (SSW-NN method).....	2
1.2 Ab-initio thermodynamics analyses	5
1.3 Optical absorption calculation.....	6
2. Benchmark of NN calculations for TiO_xH_y systems as compared with DFT results	7
3. The global PES analyses for TiO_xH_y bulks	10
4. The global PES analyses for TiO_xH_y surfaces	12
4. The HER activity exploration on amorphous $\text{TiO}_2\text{-}0.69\text{H}$ surface	14
5. XYZ positions for local minima of TiO_xH_y	15
6. Parameters for structural descriptors	20
7. References	24

1. Methodology and calculation details

1.1 Stochastic surface walking (SSW) global PES exploration using neural network (NN) potential (SSW-NN method)

a. HDNN architecture



Scheme S1. Scheme for the HDNN architecture. The subscripts i and N represent atom indices and total number of atoms in a structure. The input of a NN is a set of structural descriptors $\{G_i\}$ constructed from Cartesian coordinates $\{R\}$ of a structure, and the outputs are the atomic properties $\{E_i, F_i, S_i\}$, i.e. energy, forces and stresses. The overall properties E^{tot} , F^{tot} , and S^{tot} , can be calculated from the individual atomic contributions.

By following the previously proposed SSW-NN method,¹ this work utilized the global dataset from SSW PES exploration of TiO_xH_y systems to generate the high dimensional neural network (HDNN) potential.^{2,3} The HDNN architecture is schematically shown in Scheme S1. In Eq S1, the total energy E^{tot} can be decomposed and written as a linear combination of atomic energy E^i , which is the output of the standard neural network. The input nodes are a set of geometry-based structural descriptors, $\{G_{j,i}\}$, and are very detailed discussed in main text.

$$E^{tot} = \sum_i E_i, (S1)$$

The atomic force can be analytically derived according to Eq. S2, where the force component $F_{k,\alpha}$, $\alpha=x, y$ or z , acting on the atom k is the derivative of the total energy with respect to its coordinate $R_{k,\alpha}$. By combining with Eq. S1, the force component can be further related to the derivatives of the atomic energy with respect to j^{th} structural descriptors of atom i , $G_{j,i}$:

$$F_{k,\alpha} = -\frac{\partial E^{tot}}{\partial R_{k,\alpha}} = -\sum_{i,j} \frac{\partial E_i}{\partial G_{j,i}} \frac{\partial G_{j,i}}{\partial R_{k,\alpha}}, (S2)$$

Similarly, the static stress tensor matrix element $\sigma_{\alpha\beta}$ can be analytically derived as:

$$\sigma_{\alpha\beta} = -\frac{1}{V} \sum_{i,j,d} \frac{(r_d)_\alpha (r_d)_\beta}{r_d} \frac{\partial E_i}{\partial G_{j,i}} \frac{\partial G_{j,i}}{\partial r_d}, (S3)$$

where r_d and r_d are the distance vector constituting of $G_{j,i}$ and its module, respectively, and V is the volume of the structure.

b. Structure Descriptors

The power-type structure descriptors (SDs) are utilized to describe the geometrical environment of atom. There are six types of SDs, namely S^1 to S^6 and they have the following mathematic forms:

$$f_c(R_{ij}) = \begin{cases} 0.5 \times \tanh^3 \left[1 - \frac{r_{ij}}{r_c} \right], & \text{for } r_{ij} \leq r_c \\ 0 & \text{for } r_{ij} > r_c \end{cases} \quad (\text{S4})$$

$$R^n(r_{ij}) = r_{ij}^n \cdot f_c(r_{ij}), \quad (\text{S5})$$

$$\mathbf{S}_i^1 = \sum \text{GU}_1 = \sum_{j \neq i} R^n(r_{ij}), \quad (\text{S6})$$

$$\mathbf{S}_i^2 = \left[\sum_{m=-L}^L \left| \sum \text{GU}_2 \right|^{2\frac{1}{2}} \right]^{\frac{1}{2}} = \left[\sum_{m=-L}^L \left| \sum_{j \neq i} R^n(r_{ij}) Y_{Lm}(r_{ij}) \right|^{2\frac{1}{2}} \right]^{\frac{1}{2}} \quad (\text{S7})$$

$$\mathbf{S}_i^3 = 2^{1-\zeta} \sum \text{GU}_3 = 2^{1-\zeta} \sum_{j,k \neq i} (1 + \lambda \cos \theta_{ijk})^\zeta \cdot R^n(r_{ij}) \cdot R^m(r_{ik}), \quad (\text{S8})$$

$$\mathbf{S}_i^4 = 2^{1-\zeta} \sum \text{GU}_4 = 2^{1-\zeta} \sum_{j,k \neq i} (1 + \lambda \cos \theta_{ijk})^\zeta \cdot R^n(r_{ij}) \cdot R^m(r_{ik}) \cdot R^p(r_{jk}), \quad (\text{S9})$$

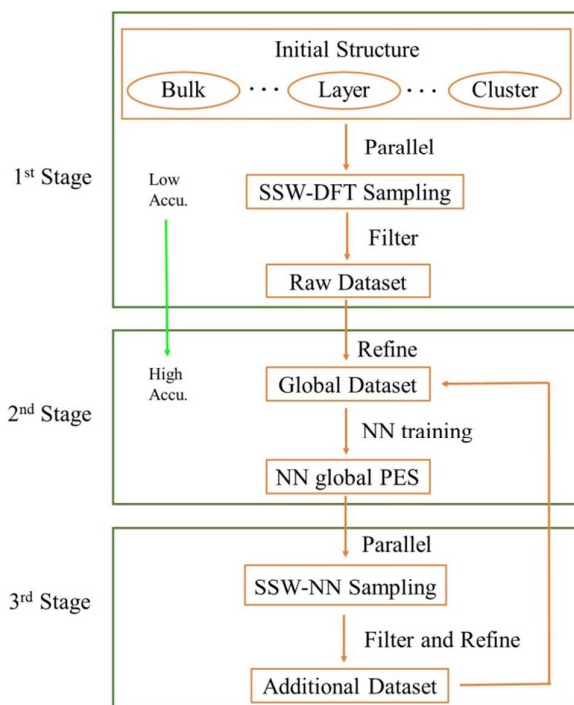
$$\begin{aligned} \mathbf{S}_i^5 &= \left[\sum_{m=-L}^L \left| \sum \text{GU}_5 \right|^{2\frac{1}{2}} \right]^{\frac{1}{2}} \\ &= \left[\sum_{m=-L}^L \left| \sum_{j,k \neq i} R^n(r_{ij}) \cdot R^m(r_{ik}) \cdot R^p(r_{jk}) \cdot (Y_{Lm}(\mathbf{r}_{ij}) + Y_{Lm}(\mathbf{r}_{ik})) \right|^{2\frac{1}{2}} \right]^{\frac{1}{2}}, \quad (\text{S10}) \end{aligned}$$

$$\mathbf{S}_i^6 = 2^{1-\zeta} \sum \text{GU}_6 = 2^{1-\zeta} \sum_{j,k,l \neq i} (1 + \lambda \cos \delta_{ijkl})^\zeta \cdot R^n(r_{ij}) R^m(r_{ik}) R^p(r_{il}), \quad (\text{S11})$$

Each SD can be considered as a sum of the n -body functions, named as the group unit (GU). The power function $R^n(r_{ij})$ represents the radial function in the GU. In the equations, r_{ij} is the distance of all atomic pairs, r_c is the cutoff, beyond which the value of Eq. 1 is equal to zero, $Y_{Lm}(r_{ik})$ is the spherical harmonic function, and n , m , p , λ and ζ are power parameters. Depending on the functional form of GU, the SDs \mathbf{S}_i^1 , \mathbf{S}_i^2 , \mathbf{S}_i^3 , \mathbf{S}_i^4 , \mathbf{S}_i^5 and \mathbf{S}_i^6 can be considered as 2-body, 3-body and 4-body functions, respectively, where the \mathbf{S}_i^2 and \mathbf{S}_i^5 involve also the spherical function. The detailed parameters of SDs are shown in Section 5 (Table S3-8).

c. Constructing global dataset using SSW-NN

The dataset used for training the NN determines largely the quality of NN PES. Our previous work has shown that the SSW global optimization can be used to fast generate a global dataset,¹ which incorporates different structural patterns on the global PES. The SSW PES search is fully automated and does not need a priori knowledge on the system, such as the structure motif (e.g., bonding patterns, symmetry) of materials. The details of SSW method can be found in previous literatures.^{4,5} The final obtained global dataset in this work, including the atom numbers, the compositions is described in Table S1. The SSW-NN method involves three stages for constructing the global dataset, as shown in Scheme S2 and the text.



Scheme S2. Procedure for generating the training dataset using SSW global optimization. At the first stage, the SSW sampling is typically calculated with low accuracy first principle calculations. At the second stage, the global dataset is first refined using high accuracy setups, followed by the NN training on the accurate global dataset. At the third stage, an additional dataset is generated by SSW sampling utilizing NN PES obtained previously. This additional dataset is then fed into global dataset (back to stage 2) and start a new cycle of NN training.

Table S1. Structure information in the first principles global dataset. Listed data are the number of the structures in the global dataset, as distinguished by the chemical formula, the number of atoms (N), the type of structures (cluster, bulk, layer).

formula	N	cluster	layer	bulk	total
O7-Ti4	11	0	45	15487	15532
O8-Ti4	12	0	0	2517	2517
H1-O8-Ti4	13	0	0	46742	46742
H1-O12-Ti6	19	0	1352	713	2065
H2	2	0	86	0	86
H2-O8-Ti4	14	941	5642	44313	50896
H2-O12-Ti6	20	0	919	534	1453
H2-O16-Ti8	26	0	7	373	380
H3-O8-Ti4	15	0	3	8547	8550
H3-O12-Ti6	21	0	1109	663	1772
H4-O4-Ti8	16	0	0	1671	1671
H4-O8-Ti4	16	104	2206	8593	10903
H4-O16-Ti8	28	0	17	1202	1219
total	--	1045	11386	131355	143786

1.2 Ab-initio thermodynamics analyses

In Figure 5, we show the phase diagram of TiO_xH_y under different H_2 temperature and pressure conditions. The diagram construction involves the computation of the reaction thermodynamics of $TiO_2 + (2 - x + y/2)*H_2 \rightarrow TiO_xH_y + (2 - x)*H_2O$ at given hydrogen partial pressure and temperature where the TiO_xH_y structures are obtained from the SSW-NN global optimization as reported.

To determine the gibbs free energy change (ΔG) per formula unit (f.u.) for the above reactions, one need to compute

$$\Delta G(p, T) = G[TiO_xH_y](p, T) + (2 - x) * \mu[H_2O](p, T) - G[TiO_2](p, T) - (2 - x + y/2) * \mu[H_2](p, T)$$

where G is the Gibbs free energy of bulks/surfaces and μ is the chemical potential for molecules. The $G[X]$ can be approximated by their DFT total energy $E[X]$ with appropriate inclusion of zero-point-energy (**ZPE**), since it is known that the vibration entropy and the pV term contributions of solid phases are negligibly small. In this work, the **ZPE** contribution of the hydroxyl group (both in bulk and on surface) is corrected by adding 0.17 eV per O-H bond, which is estimated from the phonon spectra of hydrogenated bulk phases. The chemical potential for molecules $\mu[X]$ can be calculated as follows:

$$\mu[X](p, T) = E[X] + ZPE[X] + \{H[X](p^0, T) - H[X](p^0, 0K) - TS[X](p^0, T) + k_B T \ln \frac{p}{p^0}\}$$

where enthalpy (H) and entropy (S) terms are taken from the standard thermodynamics data.

1.3 Optical absorption calculation

All optical absorption spectra were determined from first principles plane-wave DFT calculations as implemented in VASP by using the hybrid HSE06 functional. In these calculations, the imaginary part of dielectric function $\epsilon_{(2)}$ was calculated by using the expression in reference⁶ that requires the input from the conduction and valence band states. The absorption coefficient $\alpha(\omega)$ was calculated via the formula:

$$\alpha(\omega) = \sqrt{2}\omega \left(\sqrt{\epsilon_{(1)}^2(\omega) + \epsilon_{(2)}^2(\omega)} - \epsilon_{(1)}(\omega) \right)^{1/2}$$

where $\epsilon_{(1)}$ is the real part of dielectric function, which could be obtained from $\epsilon_{(2)}$ by Kramer–Kronig relationship.

2. Benchmark of NN calculations for TiO_xH_y systems as compared with

DFT results

Table S2. Benchmark of NN calculations for TiO_xH_y systems as compared with DFT results. Listed data include the compositions, total atom number (Natom), lattice type, relative DFT energy of different structures (ΔE_{DFT} , eV) which is calculated by $\Delta E_{DFT} = E[\text{TiO}_x\text{H}_y] + (2-x) * E[\text{H}_2\text{O}] - E[\text{TiO}_2] - (2-x+y/2) * E[\text{H}_2]$, energy differences between DFT energy and NN energy (E_{diff} , meV/atom) and notations. Mean error between DFT energy and NN energy is 7.88 meV/atom.

Composition	Natom	Lattice type	ΔE_{DFT}	E_{diff}	Notations
H2	2	cluster	0.000	-11.854	H ₂ molecule
H2	2	cluster	0.013	-11.636	
H2	2	cluster	0.015	-11.563	
H2	2	cluster	0.032	-10.879	
H2	2	cluster	0.046	-10.516	H ₂ molecule with different H-H bond lengths
H2	2	cluster	0.570	-13.727	
H2	2	cluster	0.607	-14.206	
H2	2	cluster	1.152	-11.631	
Ti4O8	12	bulk	0.000	-7.288	Anatase
Ti4O7	11	bulk	0.763	-3.373	
Ti4O7	11	bulk	1.049	-8.448	
Ti4O7	11	bulk	1.219	8.364	
Ti4O7	11	bulk	1.247	5.758	
Ti4O7	11	bulk	1.337	2.502	
Ti4O8	12	bulk	0.805	-11.437	
Ti4O8	12	bulk	1.222	-4.983	
Ti4O8H2	14	bulk	0.165	-8.322	
Ti4O8H2	14	bulk	0.249	-4.281	
Ti4O8H2	14	bulk	0.283	-4.985	
Ti4O8H2	14	bulk	0.306	-13.846	
Ti4O8H2	14	bulk	0.410	-6.649	
Ti4O8H3	15	bulk	2.066	-11.205	
Ti4O8H3	15	bulk	2.427	-15.535	
Ti4O8H3	15	bulk	3.217	0.263	
Ti4O8H3	15	bulk	3.344	4.242	
Ti4O8H3	15	bulk	3.378	-4.109	
Ti4O8H3	15	bulk	3.595	-0.127	
Ti4O8H3	15	bulk	3.779	-1.864	
Ti4O8H3	15	bulk	3.882	-9.518	
Ti4O8H3	15	bulk	3.988	-13.795	
Ti4O8H3	15	bulk	4.091	3.643	
Ti4O8H3	15	bulk	4.640	10.261	

Ti4O8H3	15	bulk	4.970	1.952	
Ti4O8H3	15	bulk	5.198	-8.539	
Ti4O8H3	15	bulk	5.797	-1.424	
Ti4O8H3	15	bulk	6.238	-3.838	
Ti4O8H3	15	bulk	6.362	-5.680	
Ti4O8H3	15	bulk	6.529	-12.599	
Ti4O8H3	15	bulk	9.652	-0.110	
Ti4O8H3	15	bulk	12.598	-2.869	
Ti4O8H3	15	bulk	15.583	-20.563	
Ti4O8H3	15	bulk	15.823	10.179	
Ti4O8H3	15	bulk	17.666	1.057	
Ti4O8H3	15	bulk	21.126	-2.695	
Ti4O8H3	15	bulk	23.568	0.517	
Ti4O8H3	15	bulk	27.168	2.050	
Ti4O8H4	16	layer	2.257	-12.686	
Ti4O8H4	16	layer	3.143	2.385	
Ti4O8H4	16	layer	3.157	1.626	
Ti4O8H4	16	layer	3.208	6.412	
Ti4O8H4	16	layer	3.510	0.631	
Ti4O8H4	16	layer	3.580	3.512	
Ti4O8H4	16	layer	3.620	0.742	
Ti4O8H4	16	bulk	3.989	-4.070	
Ti4O8H4	16	bulk	4.620	-7.884	
Ti4O8H4	16	bulk	4.793	-14.062	
Ti4O8H4	16	bulk	4.859	-3.919	
Ti4O8H4	16	layer	5.135	5.671	
Ti4O8H4	16	bulk	5.158	0.993	
Ti4O8H4	16	bulk	5.260	1.971	
Ti4O8H4	16	bulk	5.362	-5.484	
Ti4O8H4	16	bulk	5.463	6.180	
Ti4O8H4	16	layer	5.565	-9.602	
Ti4O8H4	16	layer	5.667	-12.912	
Ti4O8H4	16	bulk	5.769	-4.045	
Ti4O8H4	16	cluster	5.870	-6.139	
Ti4O8H4	16	bulk	5.972	20.820	
Ti4O8H4	16	bulk	6.074	11.677	
Ti4O8H4	16	cluster	6.175	4.546	
Ti4O8H4	16	bulk	6.175	-6.667	
Ti4O8H4	16	bulk	6.175	2.311	
Ti56O112	168	surface	0.000	7.844	Pristine (112) surface
Ti56O108	164	surface	2.807	-2.919	Unreconstructed TiO ₂ -0.13O _v (112) surface
Ti56O108	164	surface	7.324	3.764	Amorphous TiO ₂ -0.13O _v surface
Ti56O110	166	surface	0.803	-11.821	Unreconstructed TiO ₂ -0.25O _v (112) surface
Ti56O110	166	surface	3.085	-4.711	Amorphous TiO ₂ -0.25O _v surface

Ti56O112H1	169	surface	-0.717	-11.240	Unreconstructed TiO ₂ -0.06H (112) surface
Ti56O112H3	171	surface	-1.496	-12.801	Unreconstructed TiO ₂ -0.19H (112) surface
Ti56O112H5	173	surface	-2.015	-8.916	Unreconstructed TiO ₂ -0.31H (112) surface
Ti56O112H5	173	surface	-1.577	-11.263	Amorphous TiO ₂ -0.31H surface
Ti56O112H7	175	surface	-2.472	-9.539	Unreconstructed TiO ₂ -0.44H (112) surface
Ti56O112H7	175	surface	-1.342	-8.704	Amorphous TiO ₂ -0.44H surface
Ti56O112H9	177	surface	-2.637	-8.182	Unreconstructed TiO ₂ -0.56H (112) surface
Ti56O112H9	177	surface	-0.823	-5.633	Amorphous TiO ₂ -0.56H surface
Ti56O112H11	179	surface	-2.798	-6.590	Unreconstructed TiO ₂ -0.69H (112) surface
Ti56O112H11	179	surface	-0.028	-4.317	Amorphous TiO ₂ -0.69H surface
Ti56O112H13	181	surface	-2.008	-6.397	Unreconstructed TiO ₂ -0.81H (112) surface
Ti56O112H13	181	surface	0.932	-2.107	Amorphous TiO ₂ -0.81H surface

3. The global PES analyses for TiO_xH_y bulks

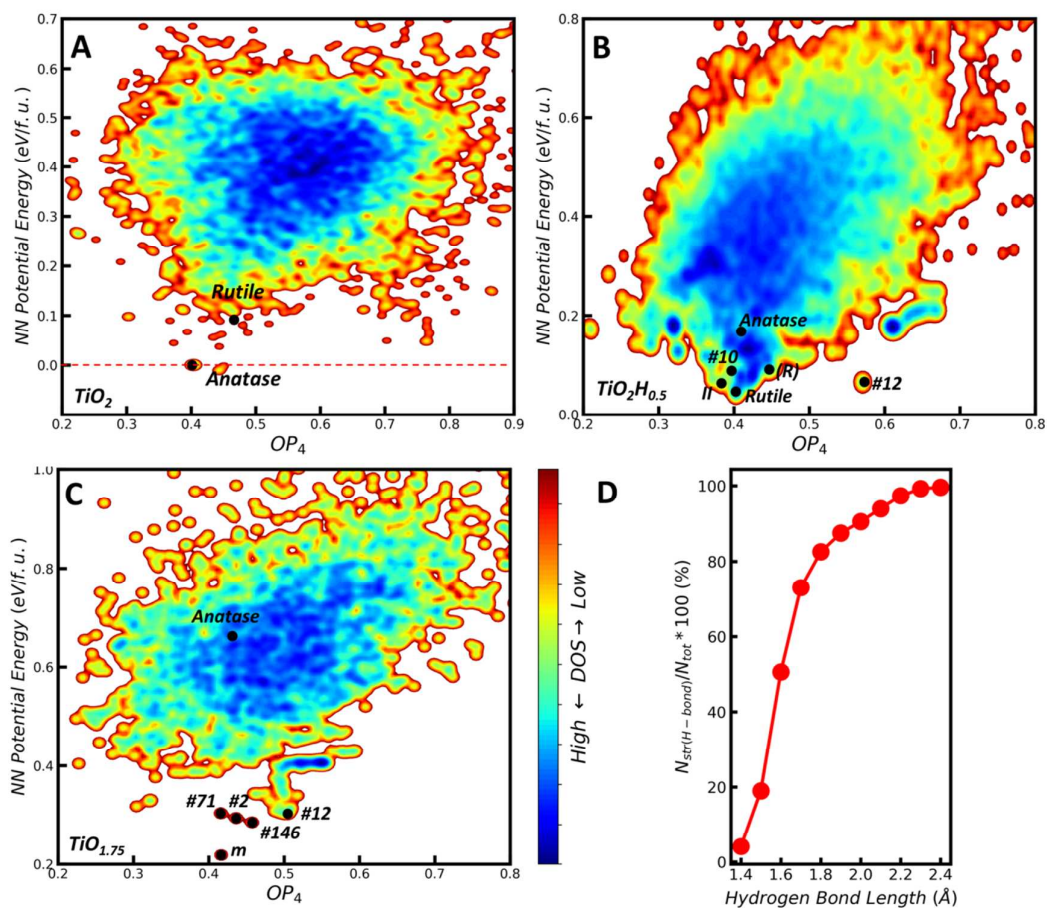


Figure S1. Global PES of (A) TiO_2 , (B) $\text{TiO}_2\text{H}_{0.5}$ and (C) $\text{TiO}_{1.75}$ with the minima from the NN-SSW global search and (D) the H-bonding distribution for $\text{TiO}_2\text{H}_{0.5}$ PES. The NN potential energy (eV/f.u.) of pure anatase TiO_2 with hydrogen gas is set as reference. The similar structures are distinguished by the OP parameter with angular momentum $L = 4$ as a fingerprint for structure. The $\text{TiO}_2\text{H}_{0.5}$ PES shows a continuous distribution of crystalline phase zone ($\Delta E < 0.10$ eV/f.u.). The next stable structures, e.g. II- ($Pbcn$, #60), #12- ($C2/m$, #12), #10- ($P2/m$, #10) and (R)-type ($Pnma$, #62) $\text{TiO}_2\text{H}_{0.5}$, are slightly less stable (~ 0.03 eV/f.u.) than the most stable rutile-type $\text{TiO}_2\text{H}_{0.5}$. The $\text{TiO}_{1.75}$ PES shows a discrete distribution of crystalline phase zone ($\Delta E < 0.35$ eV/f.u.). The next stable phase structures, e.g. #146- ($R3$, #146), #2- ($P-1$, #2), #71- ($Immm$, #71) and #12- ($C2/m$, #12) $\text{TiO}_{1.75}$, are around 0.1 eV/f.u. less stable than the m - $\text{TiO}_{1.75}$. In (D), each point represents the proportion for the number of structures with the hydrogen bonds ($N_{str(H-bond)}$) with a particular length (x-axis) relative to the number of total structures (N_{tot}) from the $\text{TiO}_2\text{H}_{0.5}$ global PES.

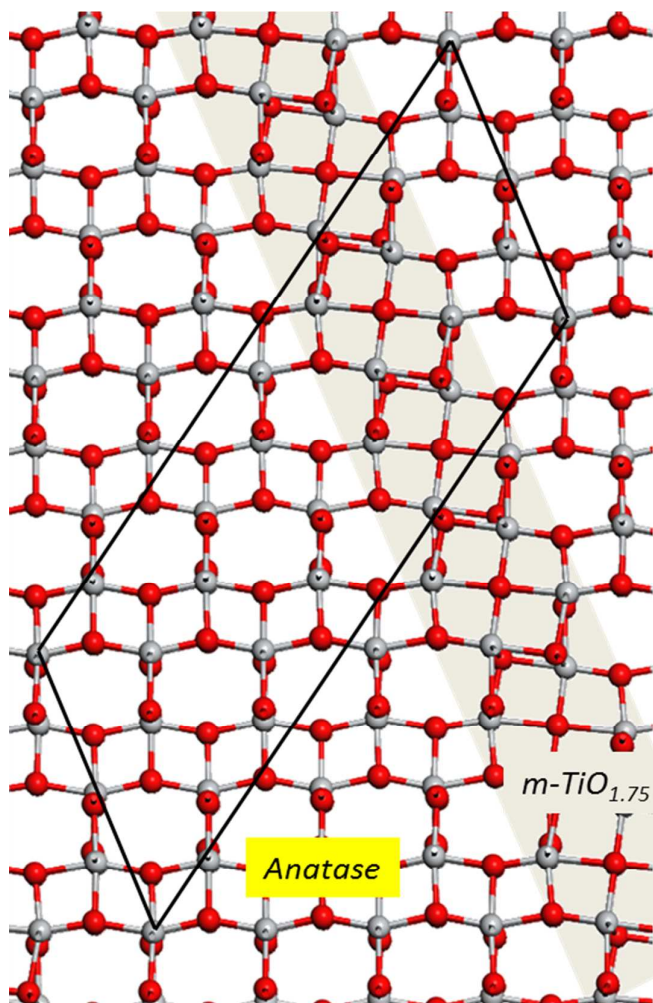


Figure S2. The global minimum of $\text{TiO}_{1.92}$, which can be regarded as a combination of anatase and m-type $\text{TiO}_{1.75}$.

4. The global PES analyses for TiO_xH_y surfaces

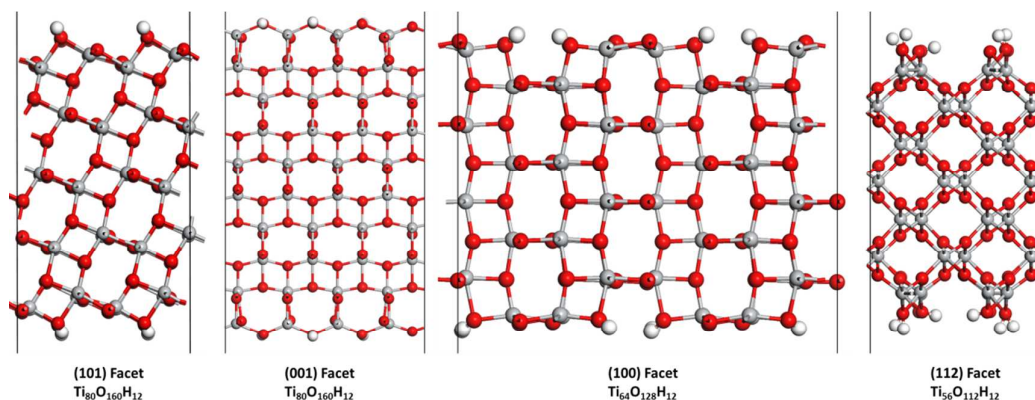


Figure S3. Pristine TiO_2 surface models with 75 % surface hydrogen coverage as the starting structure in SSW-NN PES exploration. After the SSW-NN exploration with visiting more than 10,000 minima, hydrogenated (101) and (100) surfaces maintain their initial surface Ti-O lattice structures but with a different hydrogen arrangement, while the hydrogenated (001) and (112) surfaces show an obvious structural reconstruction as shown in Figure 4.

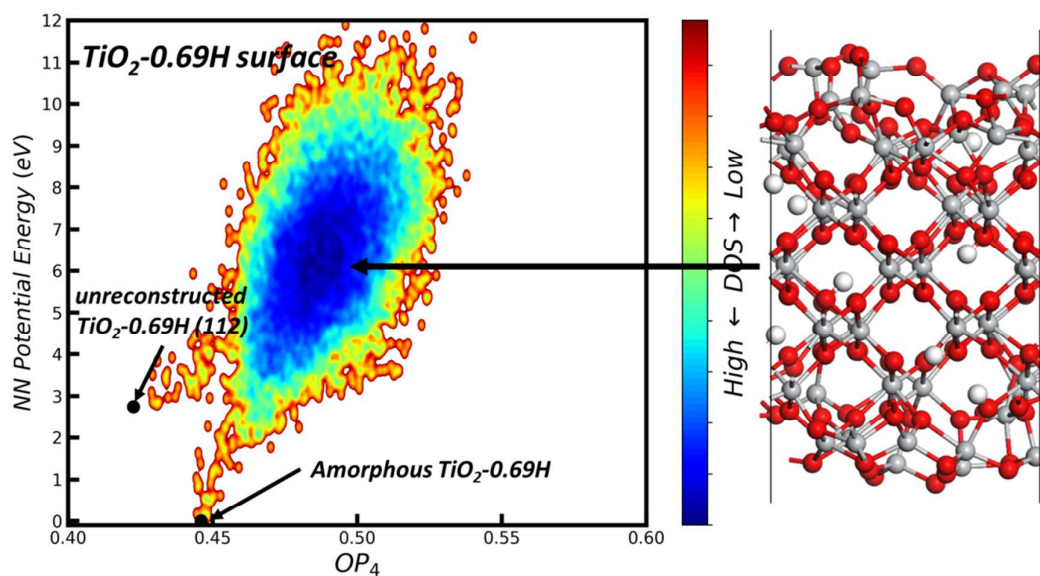


Figure S4. Global PES of $\text{TiO}_2\text{-}0.69\text{H}$ surface with more than 10,000 minima from the NN-SSW global search. The NN potential energy (eV/f.u.) of the most stable $\text{TiO}_2\text{-}0.69\text{H}$ structure is set as energy zero. The OP parameter (x -axis) with angular moment $L = 4$ is utilized to distinguish different structures. A structure with melted surfaces is also illustrated on the right, which locates in the high density region of the global PES.

Anatase TiO₂ volume per formula unit: 33.81 Å³.

Experimental TiO₂ nanoparticle size: 8 nm.

Experimental TiO₂ nanoparticle amorphous shell thickness: 1 nm.

Experimental TiO₂ nanoparticle contains about 0.25 wt% hydrogen, corresponding to H:Ti = 0.23.

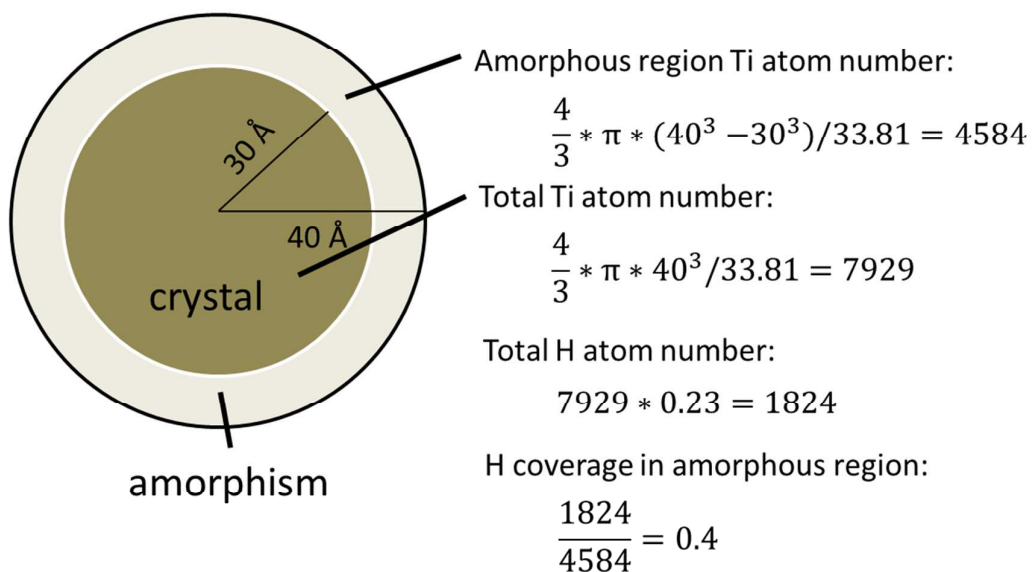


Figure S5. Estimating the H concentration in amorphous layer based on the experimental results.⁷

4. The HER activity exploration on amorphous $\text{TiO}_2\text{-}0.69\text{H}$ surface

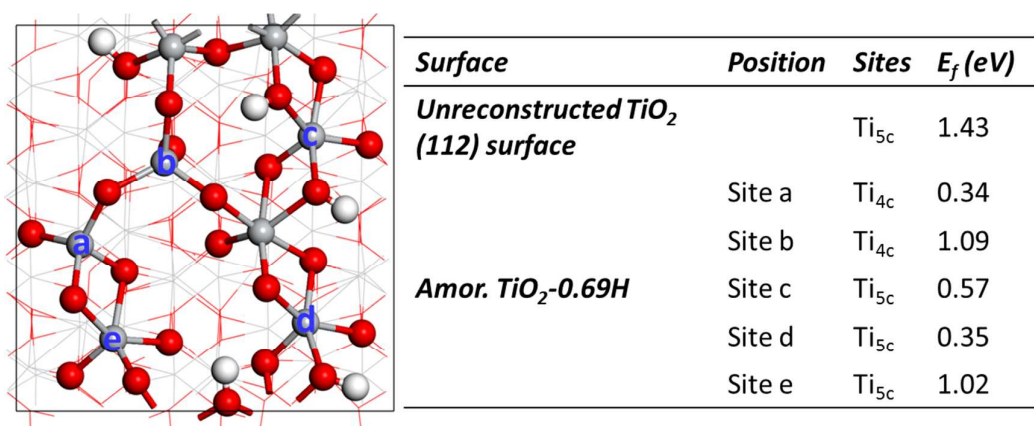


Figure S6. TiH formation energy (E_f) on different Ti sites for unreconstructed TiO_2 (112) surface and amorphous $\text{TiO}_2\text{-}0.69\text{H}$ surface.

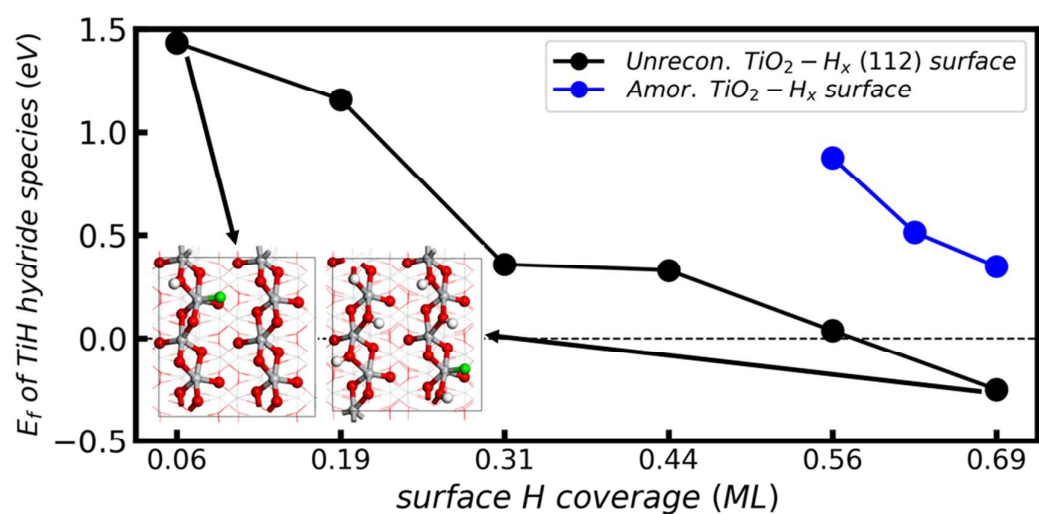


Figure S7. The formation energy (E_f) of TiH hydride species on the unreconstructed $\text{TiO}_2\text{-}H_x$ (112) surface and amorphous $\text{TiO}_2\text{-}H_x$ surface with different surface H coverage.

5. XYZ positions for local minima of TiO_xH_y

POSCAR (identified most stable amorphous TiO_2 -0.69H surface structure)

system

```
1.0000000000000000
 10.8010000000000002    0.0000000000000000    0.0000000000000000
 -0.0009262000000000    11.0556999610000002    0.0000000000000000
  0.0000000000000000    0.0000000000000000    36.0940999999999974
```

```
Ti  O  H
 56 112 11
```

Direct

```
0.1866047799633830  0.7296835998450255  0.3076122053038762
0.2973085137064370  0.4626623676682424  0.3036984708492863
0.2974463339321377  0.9628959302686575  0.3037038658847618
0.1859543871597844  0.2297115077718319  0.3077559772265305
0.6323098744362095  0.3696288524160009  0.3121359292173502
0.7836920784670641  0.6289062519061741  0.3548637587174671
0.7838360400418236  0.1287880506682312  0.3548446204857403
0.6323912033342801  0.8695582522785222  0.3120954039330571
0.5276696324917378  0.1010215164617334  0.3689408162617097
0.4183620947804687  0.8512761274517214  0.3758714519346945
0.9244065970705625  0.8550940932871287  0.3667457477511172
0.4179008548910468  0.3512093606557319  0.3759540178774365
0.5275060884286625  0.6011316020318723  0.3689009502617384
0.9232600385061218  0.3552747196975260  0.3668759265452636
0.0520659879225743  0.0923505897738669  0.3672759172459702
0.0526405745544406  0.5925599834758446  0.3672472571238021
0.7974064245420158  0.7279581601550660  0.4347241562202145
0.7965240197303538  0.2273198956167581  0.4347855865163473
0.2864199328342241  0.7216120069212740  0.4373284483863086
0.6692403392560474  0.4670054238145940  0.4362914212275867
0.6708137817203301  0.9668721020479183  0.4361365997417294
0.1639436697915840  0.4739384129961009  0.4358245134908927
0.1646627959636281  0.9732502247811712  0.4360978459470983
0.2854509914116172  0.2205008364007929  0.4372101794982946
0.9163422771784614  0.0946400707949282  0.5001438524416826
0.4186428993217733  0.0938434960933195  0.5006682669051085
0.9136430451784668  0.5960269150551177  0.4997609288617146
0.4147673804676921  0.5938304583947609  0.5006710526149249
0.0387846439476938  0.3466361821858955  0.5005150565096954
0.5355822585157529  0.3461912744505999  0.5002082514637367
0.0402634470604583  0.8453281612738419  0.5013969302578820
0.5372405055773510  0.8472210369544684  0.5003160582915295
```

0.7834691750211956	0.4677567029332581	0.5629060982727236
0.7880969909245296	0.9667620765574300	0.5654016411170060
0.2867784751415416	0.4700448370035923	0.5654650150473935
0.6670886142851908	0.2145261742635306	0.5649249885525940
0.1630327547446899	0.7163173573749417	0.5656359740104713
0.1687304309453037	0.2196912742384934	0.5639527467371928
0.6590926437345036	0.7147161067399004	0.5644460831700899
0.2878479468828694	0.9696822435094971	0.5654714471431360
0.0265886261795598	0.5943398082655897	0.6271510339864367
0.4143492182433423	0.3361054681758854	0.6301263371347529
0.9061285019184636	0.3501874114452819	0.6310769632499700
0.5338193828991705	0.0932819336363013	0.6290973969235273
0.4079830526467991	0.8330090888236714	0.6303718028082679
0.9037424485558464	0.8315359402283617	0.6291895641271003
0.5364898939585413	0.5860499397512233	0.6285835374328697
0.0333852799439766	0.1132327789508423	0.6270396739483347
0.4125426694680993	0.9436198265823733	0.7104416404138618
0.7665439239154614	0.2294003415025540	0.6911826982607787
0.6819762312302874	0.9694962327336873	0.6980562234001383
0.6477835880592840	0.4649051450790564	0.7001720842986829
0.1688901494798695	0.4326942098555387	0.6966149960082402
0.3919733601904730	0.6462888802658123	0.7121901585260533
0.2566438233431612	0.1878755444200561	0.6912150576433208
0.7818528669039624	0.7129113747268266	0.6910926522569675
0.1651393248979715	0.0573709294412292	0.3276599695561401
0.6919898118867189	0.8414435190812793	0.2643714904795914
0.6918691797053250	0.3436741767270504	0.2642831107310304
0.3027534111980535	0.1216150619748327	0.2766582917812453
0.3038350067695598	0.6214713574760347	0.2766808849402007
0.4185311082511970	0.1912601568094690	0.4000738913238283
0.7817499992982279	0.7822091740346471	0.3325676750114072
0.1935812565312015	0.3594819775833131	0.2755343443310043
0.7816635359449851	0.2821455089563372	0.3325321372198794
0.4681648040162862	0.9119853208401268	0.2828554751792534
0.4044783768298857	0.5033998644252172	0.3458933482879629
0.4678534992281597	0.4113266616365664	0.2829123180638632
0.2926502529147121	0.8109201936105112	0.3370454302561948
0.4047542019497871	0.0034658235316231	0.3458725874171422
0.9062920731055636	0.5087081237042604	0.3418726169223884
0.1939964817685509	0.8596327819093494	0.2754616379988795
0.6571486254288785	0.0264745096920508	0.3316034788215521
0.9064102906963223	0.0085266570803115	0.3417802931565520
0.6570970500027098	0.5264606317690670	0.3316640115389045
0.5385134487896328	0.7591564985136697	0.3422270579981339

0.5387201455157262	0.2591224878105825	0.3423876425795651
0.0401127158396178	0.7509192537866292	0.3371773195107524
0.0396683303320812	0.2508158745127523	0.3373009024869664
0.1648048648520093	0.5573066879160110	0.3274176357261879
0.9134696459851116	0.1854336440725014	0.3927189144177060
0.9139002977304844	0.6856545308220894	0.3925789158181285
0.4188232892384403	0.6915051948516068	0.3999714466538967
0.2924489754621608	0.3108214134105925	0.3371117534904841
0.5431502844375788	0.9462793382873758	0.3988115952740012
0.7975078595257484	0.8818990478988831	0.4057813233454968
0.5427122754750198	0.4468226436257339	0.3988732756016818
0.1655201456907587	0.1295608602927019	0.4070457416202961
0.7972371727171359	0.3816165960815576	0.4058952589948956
0.0501321836882778	0.4359481154972851	0.3944062213361177
0.2937312099772409	0.3807806274979120	0.4112521758539245
0.0502817890026055	0.9358093374986827	0.3945434967262108
0.6809766919685153	0.1305895032888726	0.3999465868421571
0.6808015256026334	0.6314342445641934	0.3997595238075357
0.1663257319880301	0.6297403163634780	0.4067285548908737
0.2933407009561991	0.8808644413619572	0.4111164966106244
0.7886245681612247	0.5695626607813643	0.4604352427271756
0.2867515168720963	0.5654689479062239	0.4637668255692095
0.7884700255344548	0.0689979513506211	0.4611287616420219
0.2871935584544080	0.0650174688088208	0.4637680175997671
0.9155432313460413	0.2531425170692359	0.4721842347268583
0.1613031104407359	0.3148899644732333	0.4627231933649334
0.9166857266460843	0.7542447486524028	0.4722705870888046
0.6661330529271099	0.8129774735906173	0.4607235565232206
0.4127858454363194	0.2521235519137402	0.4743776833380929
0.4135362028219897	0.7532040272939763	0.4740740949273010
0.6646380766798754	0.3128485500302361	0.4605250918498170
0.1619373490888157	0.8143535728884841	0.4630263827019183
0.5427105593429298	0.0021446332213857	0.4730508341988610
0.5427437371978409	0.5028491225278813	0.4735133303859586
0.0362947692542064	0.0013970853860804	0.4725536184856673
0.0361553261872569	0.5036006252691871	0.4720259875344443
0.9112566763726516	0.4386674672882333	0.5267832293184688
0.9171945854512350	0.9384722208804699	0.5289469109201544
0.2931388370194684	0.3094816972170108	0.5922039974807012
0.4162886688518520	0.9370221776131442	0.5285237870165180
0.4146152128116616	0.4372930862067509	0.5281177606777852
0.2940475095498403	0.1257369385656283	0.5390206237810654
0.7942553377953460	0.1242499159019467	0.5396509348776610
0.7870521951582131	0.6264366090665572	0.5375530831041918

0.0408637526899257	0.1885179224868530	0.5268796356526600
0.5389503191460279	0.6882106557724953	0.5275698793326118
0.0381558785479006	0.6872203709720762	0.5283409480705314
0.5436449666786330	0.1853700812848443	0.5276684818380268
0.6642807220961496	0.3721962210176381	0.5376936219856653
0.6672325784353562	0.8752297808962969	0.5385059438247547
0.1617632484031451	0.3799968185277492	0.5386903123772799
0.1670854101926652	0.8751924826664992	0.5389833910913957
0.0403932993479728	0.4605520546349024	0.6623326624877293
0.9079661667255523	0.5093948157005802	0.6027832166479751
0.6665927406782196	0.0579363119561400	0.5940037069628535
0.1674606666618411	0.5637812938878182	0.5960390695382719
0.2868112165783829	0.8096418952760074	0.5948528162115807
0.6582475423021630	0.5576095724185950	0.5913665969625175
0.1616384950273734	0.0656145600233315	0.5921452925768410
0.7896534300403052	0.3139056912033898	0.5935831451705033
0.9211858011425910	0.9939403515055876	0.6098551037745614
0.7855489485936217	0.8056648081663055	0.5942417863232730
0.2916918504229020	0.6267479767903429	0.5395923942123522
0.0458396386663549	0.7579556001585239	0.6058929001764861
0.4181451030001710	0.9904383472343263	0.6051690964258584
0.5416562174307786	0.2463084851354749	0.6044737510472455
0.0428088103962892	0.2646532634001974	0.6036810120382978
0.6626860390247866	0.3184471396137388	0.7240629342149151
0.6932841945386546	0.8155357215853077	0.7285004992566471
0.6677137134754505	0.6325640782368043	0.6651287072116434
0.4042559184208916	0.7974840186566807	0.7350174761468702
0.4047454936978518	0.1779349397534855	0.6576468828125431
0.2867199970028680	0.3624247194796188	0.6681999963549495
0.7863625170514924	0.3900642303077677	0.6692867122418648
0.9342409855742971	0.6910378109407369	0.6639288413696874
0.2410242493039583	0.5677988836222363	0.7183080840579180
0.4125133240096572	0.6797440055022479	0.6615679032575589
0.8117709126471695	0.8851846462005508	0.6731279301837219
0.5309145966135138	0.9306401752594837	0.6680945495176241
0.5581652412211949	0.0218684260324796	0.7366957335842392
0.2919889336647750	0.8958394458334956	0.6710380609867317
0.1513905625969423	0.2895576087691160	0.7211710030531224
0.7940979584586089	0.5684618174928628	0.7244446301935792
0.6590121457757939	0.1241596185294275	0.6683450993836458
0.8120469473736862	0.0881494161121232	0.7230042336477824
0.4117041515154383	0.4971100312972674	0.6041025172185238
0.5364229772717076	0.4350109451235371	0.6591761757100153
0.9152821283518761	0.2023434267397069	0.6601128170010045

0.1428297332979782	0.0908415644800761	0.6669568017657217
0.3176852991315696	0.0774382221766471	0.7243647710414196
0.5229568886545581	0.5542264715335334	0.7263676603194941
0.5365344454554023	0.7478766169450594	0.6046507528590916
0.7758371328158453	0.3118115513484520	0.2627888614184099
0.4805073181132050	0.8977298216539910	0.2564601827331715
0.4806026434718448	0.3979866335648269	0.2564895994175735
0.3769685750298909	0.1559302598392404	0.2655892761190731
0.2270748723036556	0.9575727962973066	0.6657539319655272
0.6312024206400173	0.7879713217873918	0.7462563180590228
0.7754704426972163	0.8082930804066927	0.2632202394109581
0.8704181794288790	0.5222946493003285	0.7214476587725691
0.5529889497560190	0.1048951396895245	0.7457772687238204
0.3791045477141523	0.6553940736449101	0.2661393009938455
0.8979868462937527	0.0618332743273877	0.7207494883587077

6. Parameters for structural descriptors

Table S3. Parameters of the structural descriptors S^1 (see Eq. S6) used to describe the atomic environment. r_c , nb and n are cutoff radius, neighboring atom type and power parameter, respectively. The notation, 'All', represents that these SDs do not distinguish the surrounding atom type.

No.	r_c	nb	n	No.	r_c	nb	n
1	1.9	H	8	25	4.0	H	8
2	2.3	H	2	26	5.0	H	8
3	2.8	H	4	27	6.0	H	8
4	2.6	Ti	8	28	2.6	Ti	2
5	3.0	Ti	2	29	3.0	Ti	2
6	3.6	Ti	4	30	4.0	Ti	2
7	2.0	O	8	31	5.5	Ti	2
8	2.4	O	2	32	7.0	Ti	2
9	2.8	O	4	33	2.5	Ti	8
10	2.6	All	-3	34	3.0	Ti	8
11	3.5	All	-3	35	4.0	Ti	8
12	4.5	All	-3	36	5.5	Ti	8
13	2.6	All	2	37	7.0	Ti	8
14	3.2	All	2	38	2.2	O	2
15	4.0	All	2	39	3.0	O	2
16	5.0	All	2	40	4.0	O	2
17	7.0	All	2	41	5.5	O	2
18	2.2	H	2	42	7.0	O	2
19	3.0	H	2	43	2.2	O	8
20	4.0	H	2	44	3.0	O	8
21	5.0	H	2	45	4.0	O	8
22	6.0	H	2	46	5.5	O	8
23	2.0	H	8	47	7.0	O	8
24	3.0	H	8				

Table S4. Parameters of the structural descriptors S^2 (see Eq. S7) used to describe the atomic environment. r_c is the cutoff radius, n is power parameters, L is the parameters of spherical harmonic function.

No.	r_c	nb	n	L	No.	r_c	nb	n	L
1	2.0	H	2	6	16	3.2	All	2	2
2	2.6	Ti	2	6	17	3.2	H	2	2
3	2.2	O	2	6	18	4.6	H	2	6
4	2.4	H	2	2	19	4.2	Ti	2	2
5	3.0	Ti	2	2	20	5.6	Ti	2	6
6	2.4	O	2	2	21	3.4	O	2	2
7	2.6	H	2	2	22	4.6	O	2	6
8	3.4	Ti	2	2	23	3.8	All	8	6
9	2.8	O	2	2	24	3.8	All	8	2

10	3.0	H	4	2	25	3.2	H	8	2
11	3.8	Ti	4	2	26	4.6	H	8	6
12	3.2	O	4	2	27	4.2	Ti	8	2
13	2.2	All	2	6	28	5.6	Ti	8	6
14	2.5	All	2	2	29	3.4	O	8	2
15	3.2	All	2	6	30	4.6	O	8	6

Table S5. Parameters of the structural descriptors S^3 (see Eq. S8) used to describe the atomic environment. r_c is the cutoff radius, n , m , ζ and λ are power parameters.

No.	r_c	nb1	nb2	n	m	ζ	λ
1	2.3	All	All	2	4	4	1
2	2.3	All	All	2	4	4	-1
3	2.9	All	All	1	-3	4	1
4	2.9	All	All	1	-3	4	-1
5	4.0	All	All	1	1	4	1
6	4.0	All	All	1	1	4	-1
7	3.0	H	H	2	2	8	1
8	3.0	H	H	2	2	8	-1
9	3.5	H	Ti	2	2	8	1
10	3.5	H	Ti	2	2	8	-1
11	3.5	Ti	Ti	2	2	8	1
12	3.5	Ti	Ti	2	2	8	-1
13	3.5	O	O	2	2	8	1
14	3.5	O	O	2	2	8	-1
15	3.5	Ti	O	2	2	8	1
16	3.5	Ti	O	2	2	8	-1
17	3.5	H	O	2	2	8	1
18	3.5	H	O	2	2	8	-1
19	6.5	H	H	2	2	4	1
20	6.5	H	Ti	2	2	4	1
21	6.5	Ti	Ti	2	2	4	1
22	6.5	O	O	2	2	4	1
23	6.5	Ti	O	2	2	4	1
24	6.5	H	O	2	2	4	1

Table S6. Parameters of the angular structural descriptors S^4 (see Eq. S9) used to describe the atomic environment. p is the power parameter. Also see Table S5 caption for explanations.

No.	r_c	nb1	nb2	n	m	p	ζ	λ	No.	r_c	nb1	nb2	n	m	p	ζ	λ
1	3.0	H	H	2	2	8	4	1	25	4.5	H	H	2	8	8	8	1
2	3.0	H	H	2	2	8	4	-1	26	4.5	H	H	2	8	8	8	-1
3	3.0	H	Ti	2	2	8	4	1	27	4.5	H	Ti	2	8	8	8	1
4	3.0	H	Ti	2	2	8	4	-1	28	4.5	H	Ti	2	8	8	8	-1
5	3.0	Ti	Ti	2	2	8	4	1	29	4.5	Ti	Ti	2	8	8	8	1
6	3.0	Ti	Ti	2	2	8	4	-1	30	4.5	Ti	Ti	2	8	8	8	-1
7	3.0	O	O	2	2	8	4	1	31	4.5	O	O	2	8	8	8	1
8	3.0	O	O	2	2	8	4	-1	32	4.5	O	O	2	8	8	8	-1

9	3.0	Ti	O	2	2	8	4	1	33	4.5	Ti	O	2	8	8	8	1
10	3.0	Ti	O	2	2	8	4	-1	34	4.5	Ti	O	2	8	8	8	-1
11	3.0	H	O	2	2	8	4	1	35	4.5	H	O	2	8	8	8	1
12	3.0	H	O	2	2	8	4	-1	36	4.5	H	O	2	8	8	8	-1
13	3.5	H	H	2	1	4	4	1	37	6.5	H	H	2	4	4	4	1
14	3.5	H	H	2	1	4	4	-1	38	6.5	H	H	2	4	4	4	-1
15	3.5	H	Ti	2	1	4	4	1	39	6.5	H	Ti	2	4	4	4	1
16	3.5	H	Ti	2	1	4	4	-1	40	6.5	H	Ti	2	4	4	4	-1
17	3.5	Ti	Ti	2	1	4	4	1	41	6.5	Ti	Ti	2	4	4	4	1
18	3.5	Ti	Ti	2	1	4	4	-1	42	6.5	Ti	Ti	2	4	4	4	-1
19	3.5	O	O	2	1	4	4	1	43	6.5	O	O	2	4	4	4	1
20	3.5	O	O	2	1	4	4	-1	44	6.5	O	O	2	4	4	4	-1
21	3.5	Ti	O	2	1	4	4	1	45	6.5	Ti	O	2	4	4	4	1
22	3.5	Ti	O	2	1	4	4	-1	46	6.5	Ti	O	2	4	4	4	-1
23	3.5	H	O	2	1	4	4	1	47	6.5	H	O	2	4	4	4	1
24	3.5	H	O	2	1	4	4	-1	48	6.5	H	O	2	4	4	4	-1

Table S7. Parameters of the angular structural descriptors S^5 (see Eq. S10) used to describe the atomic environment. n , m and p is the power parameter. Also see Table S4 caption for explanations.

No.	rc	nb1	nb2	L	n	m	p	No.	rc	nb1	nb2	L	n	m	p
1	2.8	H	H	2	2	2	2	19	4.5	H	Ti	2	1	8	4
2	2.8	H	H	6	2	2	2	20	4.5	H	Ti	6	1	8	4
3	2.8	H	Ti	2	2	2	2	21	3.5	Ti	Ti	2	2	4	4
4	2.8	H	Ti	6	2	2	2	22	3.5	Ti	Ti	6	2	4	4
5	2.8	H	O	2	2	2	2	23	4.5	Ti	Ti	2	1	8	4
6	2.8	H	O	6	2	2	2	24	4.5	Ti	Ti	6	1	8	4
7	2.8	O	O	2	2	2	2	25	3.5	Ti	O	2	2	4	4
8	2.8	O	O	6	2	2	2	26	3.5	Ti	O	6	2	4	4
9	2.8	Ti	Ti	2	2	2	2	27	4.5	Ti	O	2	1	8	4
10	2.8	Ti	Ti	6	2	2	2	28	4.5	Ti	O	6	1	8	4
11	2.8	Ti	O	2	2	2	2	29	3.5	O	O	2	2	4	4
12	2.8	Ti	O	6	2	2	2	30	3.5	O	O	6	2	4	4
13	3.5	H	H	2	2	4	4	31	4.5	O	O	2	1	8	4
14	3.5	H	H	6	2	4	4	32	4.5	O	O	6	1	8	4
15	4.5	H	H	2	1	8	4	33	3.5	H	O	2	2	4	4
16	4.5	H	H	6	1	8	4	34	3.5	H	O	6	2	4	4
17	3.5	H	Ti	2	2	4	4	35	4.5	H	O	2	1	8	4
18	3.5	H	Ti	6	2	4	4	36	4.5	H	O	6	1	8	4

Table S8. Parameters of the angular structural descriptors S^6 (see Eq. S11) used to describe the atomic environment. p is the power parameter. Also see Table S5 caption for explanations.

No.	rc	nb1	nb2	nb3	n	m	p	ζ	λ
1	3.0	All	All	All	2	-2	2	4	1
2	3.0	All	All	All	2	-2	2	4	-1
3	3.4	Ti	Ti	H	2	2	4	4	1

4	3.4	Ti	H	H	2	2	4	4	1
5	3.4	Ti	Ti	Ti	2	2	4	4	1
6	3.4	Ti	O	H	2	2	4	4	1
7	3.2	H	O	H	2	2	4	4	1
8	3.2	O	O	H	2	2	4	4	1
9	3.4	O	Ti	Ti	2	2	4	4	1
10	3.4	Ti	Ti	H	2	2	4	4	-1
11	3.4	Ti	H	H	2	2	4	4	-1
12	3.4	Ti	Ti	Ti	2	2	4	4	-1
13	3.4	Ti	O	H	2	2	4	4	-1
14	3.2	H	O	H	2	2	4	4	-1
15	3.2	O	O	H	2	2	4	4	-1
16	3.4	O	Ti	Ti	2	2	4	4	-1

7. References

- (1) Huang, S.-D.; Shang, C.; Zhang, X.-J.; Liu, Z.-P. Material Discovery by Combining Stochastic Surface Walking Global Optimization with a Neural Network. *Chem. Sci.* **2017**, *8*, 6327-6337.
- (2) Behler, J. Atom-centered Symmetry Functions for Constructing High-Dimensional Neural Network Potentials. *J. Chem. Phys.* **2011**, *134*, 074106.
- (3) Behler, J. Representing Potential Energy Surfaces by High-Dimensional Neural Network Potentials. *J. Phys.: Condens. Matter* **2014**, *26*, 183001-1830024.
- (4) Shang, C.; Liu, Z.-P. Stochastic Surface Walking Method for Structure Prediction and Pathway Searching. *J. Chem. Theory Comput.* **2013**, *9*, 1838-1845.
- (5) Zhang, X.-J.; Shang, C.; Liu, Z.-P. From Atoms to Fullerene: Stochastic Surface Walking Solution for Automated Structure Prediction of Complex Material. *J. Chem. Theory Comput.* **2013**, *9*, 3252-3260.
- (6) Gajdoš, M.; Hummer, K.; Kresse, G.; Furthmüller, J.; Bechstedt, F. Linear Optical Properties in the Projector-Augmented Wave Methodology. *Phys. Rev. B* **2006**, *73*, 045112.
- (7) Chen, X.; Liu, L.; Peter, Y. Y.; Mao, S. S. Increasing Solar Absorption for Photocatalysis with Black Hydrogenated Titanium Dioxide Nanocrystals. *Science* **2011**, *331*, 746-750.